Experimental and theoretical investigation of chain length and surface coverage on fouling of surface grafted polypeptoids

Andrea R. Statz, Jinghao Kuang, and Chunlai Ren
Department of Biomedical Engineering, Northwestern University, 2145 Sheridan Rd., Rm. E310, Evanston, Illinois 60208

Annelise E. Barron
Department of Bioengineering, Stanford University, W300B James H. Clark Center, 318 Campus Drive, Stanford, California 94305

Igal Szleifer[a] and Phillip B. Messersmith[b]
Department of Biomedical Engineering, Northwestern University, 2145 Sheridan Rd., Rm. E310, Evanston, Illinois 60208

(Received 19 December 2008; accepted 3 March 2009; published 21 May 2009)

Numerous strategies exist to prevent biological fouling of surfaces in physiological environments; the authors' strategy focuses on the modification of surfaces with poly-*N*-substituted glycine oligomers (polypeptoids). The authors previously reported the synthesis and characterization of three novel polypeptoid polymers that can be used to modify titanium oxide surfaces, rendering the surfaces resistant to adsorption of proteins, to adhesion of mammalian and bacterial cells, and to degradation by common protease enzymes. In this study, they investigated the effect of polypeptoid chain length on the antifouling properties of the modified surfaces. For these experiments, they used poly(*N*-methoxyethyl) glycines with lengths between 10 and 50 repeat units and determined the influence of chain length on coating thickness and density as well as resistance to protein adsorption and cellular adhesion. Short-term protein resistance remained low for all polymers, as measured by optical waveguide light mode spectroscopy, while fibroblast adhesion after several weeks indicated reduced fouling resistance for the polypeptoid-modified surfaces with the shortest chain length polymer. Experimental observations were compared to predictions obtained from a molecular theory of polymer and protein adsorption. Good agreement was found between experiment and theory for the chain length dependence of peptoid grafting density and for protein adsorption as a function of peptoid grafting density. The theoretical predictions provide specific guidelines for the surface coverage for each molecular weight for optimal antifouling. The predictions show the relationship between polymer layer structure and fouling. © *2009 American Vacuum Society.* [DOI: 10.1116/1.3115103]

I. INTRODUCTION

Inhibition of protein adsorption and cellular adhesion to surfaces is critical for proper functioning of medical devices such as cardiovascular implants,[1–3] stents,[4] and catheters.[5,6] While a variety of approaches exist for rendering surfaces resistant to fouling, immobilization of poly(ethylene glycol) (PEG) polymers is the most commonly explored method.[7–17] In order to avoid some of the reported problems associated with PEG, such as chemical or enzymatic degradation that limit long-term use in physiological environments,[18–22] researchers have developed alternative antifouling coatings including zwitterionic polymers,[23–29] polysaccharides,[30–34] and peptide mimetics.[35–38] Our strategy focuses on the use of poly-*N*-substituted glycine oligomers or polypeptoids anchored onto surfaces through a mussel adhesive-inspired peptide.[39,40] A systematic investigation of antifouling polypeptoid chain length has not previously been reported; this work should allow for interesting comparisons to be drawn between polypeptoids and numerous PEG systems.[7–17] Grafted PEG chains have been shown to exhibit increased protein resistance with increasing chain lengths. The increased fouling resistance of longer chains is explained as being due to greater excluded volumes, entropy, and steric repulsion.[15] It is not clear whether these results reflect the ability of the PEG layers to thermodynamically or kinetically control protein adsorption. As it has been shown, the role of molecular weight is very important in kinetic control; however, it plays only a secondary role in the thermodynamic control.[41–43] A similar trend is expected for polypeptoid polymers, although the chain length threshold for fouling resistance is unknown.

In this work, we investigated the influence of polypeptoid chain length on antifouling properties and further characterized the modified surfaces. The polymer thickness and surface density were compared to previous results on PEG-based systems in an attempt to better understand the packing of polypeptoid chains on surfaces. Although short-term protein fouling was found to be independent of the peptoid chain length, the shortest chain length peptoid became fouled with fibroblast cells within days, whereas the longer peptoid

[a]Electronic mail: igalsz@northwestern.edu
[b]Electronic mail: philm@northwestern.edu

chains remained cell-free for several weeks. These findings are explained with the help of theoretical predictions for the adsorption isotherms of proteins on peptoid modified surfaces. The molecular theory provides a link between the adsorption reduction and the structure of the polypeptoid layer and suggests that in the case of very short chain length, the fouling by cells is due to a kinetic effect on protein adsorption, while the surface coverage for longer peptoids is enough for the full thermodynamic protection of the surface from protein adsorption.

II. EXPERIMENTAL SECTION

A. Materials

Methoxyethylamine, tri-isopropylsilane (TIS), dimethylformamide, acetonitrile, N-morpholinopropanesufonic acid (MOPS) buffer salt, fibrinogen, 4-(2-hydroxyethyl)piperazine-1-ethanesulfonic acid (HEPES) buffer salt, tris buffer salt, sodium tetraborate, 2-propanol, 1,1′-dioctadecyl-3,3,3′,3′-tetramethylindocarbocyanine perchlorate (DiI), and alpha-cyano-4-hydroxycinnamic acid matrix were purchased from Aldrich (Milwaukee, WI). Rink amide-MBHA resin LL, Fmoc-Lys(Boc)-OH, Fmoc-Tyr(tBu)-OH, and Fmoc-DOPA(acetonide)-OH were purchased from Novabiochem (San Diego, CA). Acetic anhydride and N-methylpyrrolidone were purchased from Applied Biosystems (Foster City, CA). Trifluoroacetic acid (TFA) was obtained from Fisher Scientific (Pittsburgh, PA). Silicon wafers were purchased from University Wafer (South Boston, MA). Lyophilized whole human serum (Control Serum N) was purchased from Roche Diagnostics (Indianapolis, IN). Calcein-AM was purchased from Molecular Probes (Eugene, OR). 3T3-Swiss albino fibroblasts, Dulbecco's modified Eagle's medium (DMEM), fetal bovine serum (FBS), and penicillin/streptomycin were obtained from American Type Culture Collection (Manassas, VA). Ultrapure water (UP H_2O) used for all experiments was purified (resistivity of $\geq$18.2 MΩ cm; total organic content of $\leq$5 ppb) with a NANOpure Infinity System from Barnstead/Thermolyne Corp. (Dubuque, IA).

B. Synthesis of peptidomimetic polymers

The peptidomimetic polymers were synthesized, as described previously,[36,37] using a C S Bio 036 (C S Bio Co., Menlo Park, CA) automated peptide synthesizer. The five polymers of varying chain lengths were synthesized in one batch by removing portions of the resin from the reaction vessel at the appropriate coupling step. The C-terminal DOPA-Lys-DOPA-Lys-DOPA peptide anchor was first synthesized on a low loading rink amide resin using conventional Fmoc strategy of solid-phase peptide synthesis; the polypeptoid portion was then synthesized using a submonomer protocol.[44] The Tyr polymer analog was synthesized according to the same procedure but using Fmoc-Tyr(tBu)-OH instead of Fmoc-DOPA(acetonide)-OH. Acetic anhydride was used to acetylate the N-terminus of the polypeptoid chain upon removal from the vessel; cleavage of the polymers from the resin and deprotection of the amino acid side chains was accomplished by treating the resin with 95% (v/v) TFA, 2.5% H_2O, and 2.5% TIS for 20 min. The cleaved polymer was then removed by filtering and rinsing several times with TFA, and the solvent was removed using a rotary evaporator; the oily product was dissolved in 50/50% water/acetonitrile, frozen, and lyophilized. The crude products were purified by preparative reversed-phase high performance liquid chromatography (RP-HPLC) (Waters, Milford, MA) using a Vydac C18 column, and purified fractions were frozen and lyophilized. The purity of each final product was confirmed by RP-HPLC and matrix-assisted laser desorption/ionization mass spectrometry (MALDI-MS) (Voyager DE-Pro, Perspective Biosystem, MA).

C. Surface modification

Silicon wafers were coated with a 20-nm-thick layer of TiO_2 by electron beam evaporation (Edwards Auto306; $<10^{-5}$ Torr), and the coated wafers were cut into 8×8 mm^2 pieces. The substrates were cleaned ultrasonically for 10 min in 2-propanol and dried under N_2. Surfaces were then exposed to O_2 plasma (Harrick Scientific, Ossining, NY) at $\leq$150 Torr and 100 W for 3 min. Optical waveguide light mode spectroscopy (OWLS) waveguides were purchased from MicroVacuum Ltd. (Budapest, Hungary) and coated with a 10-nm-thick layer of TiO_2 by electron beam evaporation as described above. Sensors were cleaned following the same procedure as TiO_2 substrates. After use, OWLS waveguides were regenerated for subsequent use by 10 min sonication cycles in 0.1*M* HCl, UP H_2O, and 2-propanol, followed by exposure to O_2 plasma to remove adsorbates.

Unless otherwise noted, the general approach used for surface modification involved immersion of clean substrates and sensors in a 0.3 mM solution of peptidomimetic polymer in buffer A (3*M* NaCl buffered with 0.1*M* MOPS, *p*H=6) at 50 °C for 24 h. After modification, substrates were extensively rinsed with UP H_2O to remove any unbound polymer and then dried in a stream of filtered N_2.

D. Surface characterization

1. Spectroscopic ellipsometry measurements

Prior to modification, substrates were cleaned as described above and measured using an M-2000 spectroscopic ellipsometer (J.A. Woollam, Lincoln, NE). Measurements were made at 65°, 70°, and 75° using wavelengths from 193 to 1000 nm. After modification, substrates were rinsed and dried as described above and measured again. The spectra were fit with multilayer models in the WVASE32 software (J.A. Woollam). Optical properties of the substrate were fit using a standard TiO_2 model, while properties of the polymer layer were fit using a Cauchy model (A_n=1.45, B_n=0.01, C_n=0).[45] The obtained ellipsometric thicknesses represent the "dry" thickness of the polymer under ambient conditions. The average thickness and standard deviation of three or more substrates are reported for each polymer.

2. OWLS

For *in situ* polymer-adsorption experiments, TiO_2 coated waveguide sensors were cleaned and inserted into the measurement head of an OWLS110 (MicroVacuum Ltd.) and exposed under static conditions to buffer A through the flow-through cell (16 μl volume) for at least 24 h to allow for equilibration. The measurement head was mounted on the sample chamber and heated to 50 °C; the signal was recorded to ensure a stable baseline. Polymer solution (1 ml total volume) was injected into the flow-through cell in stop-flow mode. The waveguide sensor was exposed to the polymer solution for 4 h, subsequently rinsed with buffer A (2 ml), and allowed to equilibrate for another 30 min. Adsorption experiments with varying polymer concentrations were conducted in UP H_2O at 25 °C using the same procedure.

The measured incoupling angles, α_{TM} and α_{TE} were converted to refractive indices N_{TM} and N_{TE} by the MICROVACUUM software, and changes in the refractive index at the sensor surface were converted to adsorbed mass using de Feijter's formula.[46] The refractive indices of solutions were measured using a refractometer (J157 Automatic Refractometer, Rudolph Research) under identical experimental conditions. A refractive index value of 1.356 16 was used for buffer A, and a value of 0.129 cm^3/g was used for dn/dc in the polymer-adsorption calculations.

3. Atomic force microscopy

Atomic force microscopy (AFM) measurements were performed on an Asylum MFP-3D instrument (Asylum Research, Santa Barbara, CA) installed on a Nikon TE2000 microscope. Silicon cantilevers (VISTAprobes, T300) were used for tapping-mode measurements in air and silicon nitride cantilevers (Veecoprobes, DNP-S20) were used for tapping-mode measurements in UP H_2O.

4. X-ray photoelectron spectroscopy

Survey and high-resolution x-ray photoelectron spectroscopy (XPS) spectra were collected on an Omicron ESCALAB (Omicron, Taunusstein, Germany) configured with a monochromated Al $K\alpha$ (1486.8 eV) 300 W x-ray source, 1.5 mm circular spot size, a flood gun to counter charging effects, and an ultrahigh vacuum ($<10^{-8}$ Torr). The takeoff angle was fixed at 45°. Substrates were mounted on standard sample studs using double-sided Cu adhesive tape. Spectra were fitted using CASAXPS software; specifically a Shirley background subtraction and the sum of 90% Gaussian and 10% Lorentzian function were used. Atomic sensitivity factors were used to normalize peak areas from high-resolution spectra to intensity values, which were then used to calculate atomic compositions.[47]

E. Protein adsorption experiments

Lyophilized human serum was reconstituted in water to reach the typical concentration in blood; fibrinogen from human plasma was dissolved at 3 mg/ml concentrations in buffer B (10 mM HEPES, 150 mM NaCl, pH=7.4). For *in situ* protein-adsorption experiments, TiO_2 coated waveguide sensors were modified with peptidomimetic polymers as explained previously. After equilibration of the OWLS baseline in buffer B, protein solution was injected and allowed to adsorb for 20 min at 37 °C before rinsing with buffer B. A refractive index value of 1.331 27 was used for buffer B, and a standard value of 0.182 cm^3/g was used for dn/dc in the protein-adsorption calculations.[15]

F. Mammalian cell adhesion experiments

3T3-Swiss albino fibroblasts were maintained at 37 °C and 5% CO_2 in DMEM containing 10% FBS and 100 U/ml of penicillin/streptomycin. Immediately before use, fibroblasts of passage 12–16 were harvested using 0.25% trypsin-EDTA, resuspended in DMEM with 10% FBS, and counted using a hemacytometer. Modified and unmodified substrates were placed in a 12-well tissue culture polystyrene plate and sterilized by exposure to UV light for 10 min, after which 1 ml of DMEM containing FBS was added to each well and incubated for 30 min at 37 °C and 5% CO_2. For the long-term experiment, the fibroblast cell suspension was diluted, and the cells were seeded on each substrate at a density of 2.9×10^3 cells/cm^2 and substrates were reseeded twice per week. For live cell staining, the medium was aspirated from each well to remove any nonadherent cells and phosphate buffered saline (PBS) was used to rinse the substrates and wells. Fibroblasts were stained with 2.5 μM calcein-AM in complete PBS for 1 h at 37 °C; substrates were transferred to new culture plates with fresh media and imaged weekly. After imaging, substrates were reseeded and placed back into the incubator; media were changed every 3 days. For short-term 4 h assays on varying surface chemistries, cells were plated at a density of 29×10^3 cells/cm^2; adherent cells were fixed in 3.7% *para*-formaldehyde for 5 min and stained with 5 μM DiI for epifluorescent microscope counting.

Quantitative cell attachment data were obtained by acquiring nine images (10× magnification) from random locations on each substrate using a Leica epifluorescent microscope (W. Nuhsbaum Inc., McHenry, IL) equipped with a SPOT RT digital camera (Diagnostics Instruments, Sterling Heights, MI). Three identical substrates for each experiment were analyzed for statistical purposes, resulting in a total of 27 images per time point for each modification. The microscopy images were quantified using thresholding in Metamorph (Molecular Devices, Downingtown, PA).

G. Theoretical approach

The theoretical approach that we apply is a molecular theory that has been shown to provide accurate information as compared to experimental observations for the structure and thermodynamics of tethered polymer layers[48] as well as in the determination of the amount of protein adsorption on surfaces with grafted PEG. The agreement with experimental observations is for oligomeric chains[42] as well as long polymers[49] and at all polymer-grafting densities. Thus, we believe that the approach is very appropriate to predict the

amount of grafted polypeptoid end-adsorbed as well as the ability of the peptoid to prevent protein adsorption.

We present a simple version of the theory to highlight the main points and refer the reader to Refs. 43, 50, and 51 for a more detailed discussion and for technical details. The basic idea of the theory is to consider conformations of the chain molecules (the end tethered polypeptoids and the proteins) and by minimization of the system's free energy determine the probability of each of those conformations depending upon the solution conditions. In this way, the theory enables the study of both structural and thermodynamic properties for the explicit molecular system studied. We first derive the theory to study the amount of peptoid that adsorbs to the surface and then generalize it for the understanding of protein adsorption for surfaces with tethered polypeptoids.

Consider first a surface of total area A, with N_g end-tethered polypeptoids in contact with water. The surface coverage of polymers is defined by $\sigma=N_g/A$. The total Helmholtz free energy per unit area of the surface is given by

$$\frac{\beta F}{A}=\sigma\sum_{\alpha}P(\alpha)\ln P(\alpha)+[\sigma\ln(\sigma\Lambda^2)-\sigma]+\int dz\rho_w(z)\times[\ln\rho_w(z)v_w-1]+\int dz\frac{\chi}{v_w}\phi_p(z)^2+\int dz\beta\pi(z)\times[\phi_p(z)+\phi_h(z)+\phi_w(z)-1]+\sigma\beta F_{\text{binding}} \tag{2.1}$$

with $\beta=1/kT$ where k is the Boltzmann constant and T is the absolute temperature. The first term in the free energy represents the conformational entropy of the peptoids, with $P(\alpha)$ being the probability of finding the peptoid in conformation α. The second term is the two-dimensional (surface) translational entropy of the peptoids, with $\Lambda=(h^2/2pmkT)^{1/2}$ representing the peptoids de Broglie wavelength, where h is the Planck constant and m is the peptoid's mass. The third term represents the position dependent translational (mixing) entropy of the water (solvent) molecules, with $\rho_w(z)$ being the position dependent water density and v_w is the molecular volume of a water molecule. The fourth and fifth terms represent the attractive and repulsive intermolecular interactions with χ measuring the strength of the peptoid-peptoid attractions and $\pi(z)$ being the self-consistently determined strength of the repulsions, arising from excluded volume interactions; $\phi_i(z)$ represent the position dependent volume fraction of species $i=p$, h, and w for peptoid tail, head, and water, respectively. The last term in the free energy expression represents the bare adsorption free energy, where F_{binding} is the total strength of the free energy of binding between the pentapeptide (DOPA-Lys-DOPA-Lys-DOPA sequence) and the surface.

The probability of chain conformations as well as the position dependent solvent density is determined by the minimization of the free energy. This yields

$$P(\alpha)=\frac{1}{q}\exp\left\{-\int\vec{dz}\beta\pi(z)[n(\alpha,z)v_p+v_h(z)]-\int dz\frac{2\chi}{v_w}\phi_p(z)n(\alpha,z)v_p\right\}. \tag{2.2}$$

where q is the normalization constant, the first (second) integral in the Boltzmann factor arises from the repulsive (attractive) interactions between the polymer in conformation α and the other molecules in the system. $n(\alpha,z)dz$ represents the number of peptoid segments that the molecule in conformation α has in between z and $z+dz$, while $v_h(z)$ represents the volume that the head-group (pentapeptide) occupies at z. For the solvent volume fraction the minimization yields

$$\phi_w(z)=\rho_w(z)v_w=\exp[-\beta\pi(z)v_w]. \tag{2.3}$$

The only unknowns are the position dependent repulsive interactions, $\pi(z)$, which are determined by the constraint that at all distances from the surface, z, polymer or solvent must occupy the total volume. (See Refs. 43, 50, and 51 for the technical details of how the chain conformations are generated and the equations solved.)

To determine the amount of peptoid that end-tethers to the surface, we need to determine the surface coverage that corresponds to the same chemical potential as the peptoid in the solution. The chemical potential of the end-tethered molecules is determined by taking the appropriate derivative of the free energy [Eq. (2.1)] with respect to the number of peptoids.[51] This yields

$$\beta\mu=-\ln q+\ln\sigma+2\ln\Lambda+\beta F_{\text{binding}}, \tag{2.4}$$

which is readily calculated once the $\pi(z)$ is determined. The bulk chemical potential is given by

$$\beta\mu_b=-\ln M_b+\ln\rho_p+3\ln\Lambda-\frac{(N-1)v_p+v_h}{v_w}\ln(1-\phi_p-\phi_h)+\frac{\chi}{v_w}2\phi_p(N-1)v_p, \tag{2.5}$$

where M_b is the total number of generated chain conformations in bulk and the other quantities have been defined. Note that in Eq. (2.5) ϕ_i represents the bulk volume fraction of species i.

The amount of polymer adsorbed, through the peptapeptide-surface binding attraction F_{binding}, is determined for each molecular weight of polypeptoid using the following procedure. The chemical potential of the polymer on the surface is calculated as a function of the surface coverage and the σ for which the chemical potential has the same value as that of the bulk, determined through Eq. (2.5), corresponds to the bound amount.

The adsorption of the protein as a function of the amount of tethered polymers is determined using a generalization of the theory presented above. The details can be found in Refs. 43, 50, and 51 here we present the basic ideas. We consider a surface with grafted polymers at a surface coverage σ, with σ_{pro} as the adsorbed proteins. The free energy of the system is given by

$$\frac{\beta F}{A} = \sigma \sum_{\alpha} P(\alpha) \ln P(\alpha) + \sigma(\ln \sigma \Lambda^2 - 1) + \sigma_{\text{pro}} \sum_{\gamma} P_{\text{pro}}(\gamma) \times [\ln P_{\text{pro}}(\gamma) + \beta \varepsilon_{\text{ads}}(\gamma)] + \sigma_{\text{pro}}(\ln \sigma_{\text{pro}} \Lambda_{\text{pro}}^2 - 1) + \int dz \rho_w(z)[\ln \rho_w(z) v_w - 1] + \int dz \frac{\chi}{v_w} \phi_p^2(z) + \int dz \beta \pi(z)[\phi_p(z) + \phi_h(z) + \phi_{\text{pro}}(z) + \phi_w(z) - 1], \quad (2.6)$$

where the only difference with Eq. (2.1) is the addition of the third and fourth terms, which correspond to the protein contributions, including the conformational entropy, the adsorption energy of proteins in conformation γ, and the translational entropy of the adsorbed proteins, respectively. $P_{\text{pro}}(\gamma)$ is the probability of finding the adsorbed protein in conformation γ and $\varepsilon_{\text{ads}}(\gamma)$ is the bare adsorption energy of the protein in that conformation. We minimize the free energy and obtain the expressions for the probability distribution function of the polymer and the protein and the volume fraction distribution, $\phi_i(z)$, for each molecular species i. From the minimized free energy, the probability of the adsorbed protein conformation is given by

$$P_{\text{pro}}(\gamma) = \frac{1}{q_{\text{pro}}} \exp\left[- \beta \varepsilon_{\text{ads}}(\gamma) - \int dz \beta \pi(z) v_{\text{pro}}(\gamma, z) \right] \quad (2.7)$$

and the adsorbed proteins chemical potential is related to the amount of proteins adsorbed by

$$\sigma_{\text{pro}} = \frac{\exp(\beta \mu_{\text{pro}})}{\Lambda_{\text{pro}}^2} q_{\text{pro}}. \quad (2.8)$$

The adsorption isotherms, i.e., the amount of proteins adsorbed as a function of the surface coverage of grafted polypeptoids, are obtained by finding at each grafted polymer surface coverage the amount of adsorbed proteins that has a chemical potential equal to that of the bulk solution, which is given by $\beta\mu_{\text{pro}} = \ln(\rho_{\text{pro}}\Lambda_{\text{pro}}^3) - (v_{\text{pro}}/v_w)\ln \phi_w - \ln 2$.

The details of how the calculations are carried out can be found in Refs. 43, 50, and 51. The model for fibrinogen is identical to the one we used in earlier work, which provided good agreement for the adsorption of the proteins on PEG layers[41,43,49] and which properly accounts for the size and shape of this complex protein. We assume that the protein can adsorb in either on-flat or edge configurations and the bare free energy with the TiO_2 surface is $-305k_BT = -732$ kJ/mol and $-762.5k_BT = -1830$ kJ/mol, respectively. These values were chosen so as to get the right amount of protein adsorbed in the bare TiO_2 surface. The peptoid conformations are generated by using a coarse grained model in which each peptoid is considered within a united atom model and the volume of each peptoid is given by 0.09 nm^3, while that of the penptapeptide is 0.27 nm^3. The value of the interaction parameter is $\chi = -70/T$, where T is the absolute temperature. At room temperature, water is a good solvent for the polymer. The peptapeptide is assumed to be on the surface and therefore has no conformational degrees of freedom. For each polypeptoid chain length, we generate 10^6 independent conformations. Each conformation provides a set of volume distributions, $n(\alpha, z)v_p$ for all z, which is used in all the calculations. The equations that we solve correspond to the packing constraints, e.g., for the protein-adsorption case this is

$$\langle \phi_{\text{pol}}(z) \rangle + \langle \phi_{\text{pro}}(z) \rangle + \phi_w(z) = \sum_{\alpha} P(\alpha) n(\alpha; z) v_p + \sum_{\gamma} P_{\text{pro}}(\gamma) v_{\text{pro}}(\gamma; z) + \exp[-\beta \pi(z) v_w] = 1 \quad \text{for all } z \geq 0, \quad (2.9)$$

where the pdfs are replaced from Eqs. (2.2) and (2.7). The equations are solved by discretizing space in the form described in detail in Refs. 43, 50, and 51.

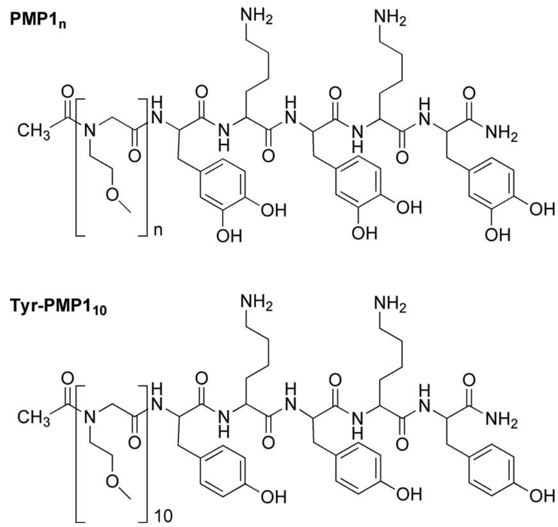

FIG. 1. Chemical structures of peptidomimetic polymers ($PMP1_n$), where $n = 10$, 15, 20, 30, or 50 and Tyr-$PMP1_{10}$.

III. RESULTS AND DISCUSSION

The polypeptoid polymers investigated in this study were designed based on the superior performance of PMP1, a peptidomimetic polymer consisting of a DOPA, and lysine pentapeptide anchor coupled to 20 *N*-methoxyethyl glycine residues.[36,37] The chemical structures of the polymers with varying chain lengths ($PMP1_n$) are shown in Fig. 1. The importance of the DOPA residues in the pentapeptide was revealed through a polymer analog that contained tyrosine residues in place of the DOPA residues in the pentapeptide anchor coupled to 10 *N*-methoxyethyl glycine residues (Tyr-$PMP1_{10}$); the structure of this polymer is also shown in Fig. 1. Characterization data (RP-HPLC and MALDI-MS) for the purified polymers are shown in the supporting information (Figs. S1 and S2).[52]

TABLE I. Polymer coating thickness measured by ellipsometry for polymer-modified TiO_2 substrates.

Substrate	Coating thickness (Å)
$PMP1_{10}$	28.5 ± 3.5
$PMP1_{15}$	32.5 ± 4.3
$PMP1_{20}$	33.6 ± 4.6
$PMP1_{30}$	34.1 ± 3.5
$PMP1_{50}$	41.5 ± 5.1
Tyr-$PMP1_{10}$	3.7 ± 0.6

TABLE II. Polymer mass adsorption measured by OWLS with corresponding molecular weights (M_w) and calculated density of polymer chains (σ).

Polymer	Adsorbed mass (ng/cm^2)	M_w	σ ($\#/nm^2$)
$PMP1_{10}$	359.7 ± 17.7	2003	1.08
$PMP1_{15}$	412.0 ± 67.6	2578	0.96
$PMP1_{20}$	456.0 ± 77.9	3156	0.87
$PMP1_{30}$	510.0 ± 24.6	4304	0.71
$PMP1_{50}$	552.3 ± 14.6	6610	0.50
Tyr-$PMP1_{10}$	50.7 ± 8.3	1956	0.16

A. Surface characterization

The polymers were adsorbed onto TiO_2 substrates from buffer A at 50 °C, corresponding to the previously reported marginal solvation conditions for $PMP1_{20}$, which allow for greater grafted polymer density by reducing chain repulsion.[36,37,53,54] While these adsorption conditions may not be optimal for all other chain lengths in the study, for experimental consistency, this modification condition was used for all experiments. The thicknesses of the polymer coatings adsorbed onto the TiO_2 surfaces as measured by spectroscopic ellipsometry are reported in Table I. Average thickness values for the polymer-modified surfaces appear to increase with number of peptoid residues, but statistically significant differences ($p < 0.02$) are detected only between $PMP1_{50}$ substrates and the shorter polymers, suggesting that small increases in chain length do not have a measurable effect on polymer thickness. The Tyr-$PMP1_{10}$ modified substrates had a significantly ($p < 0.02$) thinner polymer coating compared to all DOPA-containing polymers, suggesting that either the polymer was not able to adsorb to the substrate or the adhesive strength was weak and the polymer was easily displaced by subsequent rinsing and drying steps. Reduction in the interaction strength is expected for the tyrosine-containing polymers compared to the DOPA-containing polymers based on AFM experiments, which demonstrated that the strong interactions between DOPA and TiO_2 surfaces were much higher than the interaction strength of tyrosine and TiO_2 surfaces.[55]

Polymer adsorption was also characterized by *in situ* OWLS adsorption. This technique allows for highly sensitive (<0.5 ng/cm^2) measurement of mass adsorption per area in a flow-through cell device.[56,57] Average mass results for three independent experiments for adsorption of each polymer on TiO_2-coated waveguides are shown in Table II. As suggested by ellipsometry results, the mass of the polymer coating increases with increasing chain length and is significantly lower for Tyr-$PMP1_{10}$. These mass adsorption values were used to determine the surface density of polymer chains (σ) using the following equation:

$$\sigma = \frac{N_A m_A}{M_w},$$

where N_A is Avogadro's number, m_A is the measured mass of adsorbed polymer (in g/nm^2), and M_w is the molecular weight of the polymer. While longer chain length polymers result in greater mass adsorption, this correlates to decreased surface density of polymer chains on the surface. A decrease in the polymer density does not appear to decrease fouling resistance, most likely because the longer chains allow more peptoid units to pack in each area. As the polymer surface coverage increases, a decrease in protein adsorption should be seen due to the steric barrier from the polymer layer that the adsorbing proteins encounter.[51]

The polypeptoid backbone structure varies significantly from that of PEG; therefore, similar calculations for radius of gyration and molecular spacing cannot be made using the same parameters that are reported for PEG in literature.[10,12,14,15] However the polymer surface densities can be compared among different polymer systems in order to attempt to better understand fouling resistance of such coatings. PEG-containing surface coatings investigated by Malmsten *et al.*[14] ranged in layer thickness from 2 to 22 nm and chain density from 0.004 to 0.12 chains/nm^2 for either covalently grafted or strongly adsorbed polymers. The PLL-*g*-PEG system used on Nb_2O_5 substrates achieved surface densities of 0.9, 0.5, and 0.3 chains/nm^2 for 1, 2, and 5 kDa PEGs.[15] Comparisons of PMP1 polymer densities to equivalent mass PEGs suggest that the PMP1 polymers are able to adsorb at nearly twice the density of the PLL-*g*-PEG system. The surface density of mPEG-$DOPA_3$ neared 50 EG/nm^2 ($\sim$0.44 chains/nm^2 for PEG-5000), with a threshold for protein adsorption demonstrated around 15–20 EG/nm^2 ($\sim$0.13–0.18 chains/nm^2).[10] Thus the poor fouling resistance of the Tyr-$PMP1_{10}$ substrates should be expected with a polymer density of 0.16 chains/nm^2. Molecular spacing calculations indicated that the surface-bound mPEG-$DOPA_3$ chains were in a brushlike structure at these high surface densities;[10] the structural conformation of the polypeptoid polymers has not been determined, but a similar brushlike structure is expected, as it is shown by the predictions of the theory (see Fig. 5). The surface density results for the polypeptoid polymers are relatively high compared to PEG systems, suggesting that the MAP-inspired anchoring strategy allows for strong attachment to TiO_2 and formation of densely packed polymer layers.

To more closely study the adsorption of the polypeptoid polymers onto TiO_2 substrates, experiments were conducted using a range of polymer concentrations for $PMP1_{10}$ in H_2O. Surface density is plotted as a function of polymer concen-

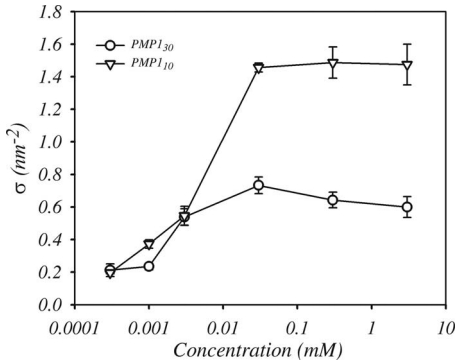

FIG. 2. Polymer chain density as a function of polymer solution concentration for PMP1$_{10}$ in UP H_2O.

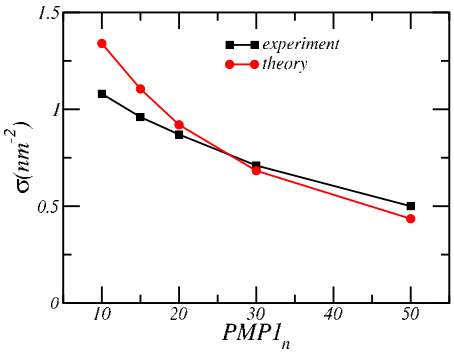

FIG. 3. (Color online) Experimental and predicted polymer surface densities as a function of the chain length of the polypeptoid.

tration in Fig. 2. Results indicate that the density increases with concentration but appears to level off at higher concentrations.

The next step is to compare the predictions from the molecular theory with the measured amount of polypeptoid on the surface (Table II). To this end, Fig. 3 shows the amount of polymer adsorbed as a function of the length of the peptoid. The predictions of the theory are in good agreement with the experimental observations. The trends are identical in both cases, i.e., the amount of polypeptoid adsorbed decreases as the peptoid chain length increases. This result is not unexpected since the anchoring group, the DOPA-Lys pentapeptide, is identical in all cases and therefore the driving force for binding to the surface should be the same. However, as the chain length increases, the repulsions between the peptoids increases and thus less polymer can be attached with the same driving force. Interestingly the theory predictions are worst at the shortest chain length, indicating that in these cases, a more detailed model for the peptoids may be necessary. We are working in that direction; however, it is clear that the main trends of the adsorption are nicely captured by the theory.

To better understand the surface architecture of polymer-modified surfaces, tapping-mode AFM was used to image PMP1$_{50}$ substrates under dry and aqueous conditions (Fig. 4). The dry substrate had an average rms roughness of 161 ± 58 pm, and the roughness of the wet substrate was similar (rms roughness of 193 ± 8 pm). These low roughness values and images demonstrate that homogeneous polymer layers can be created using these polypeptoid polymers. Similar roughness values were reported for PEG surfaces on glass.[11] To determine the hydrated thickness of the polymer coatings, a scratch was made in the coating using a clean surgical blade, and then the area was imaged using tapping mode. The change in height between the scratched surface and the polymer coating was assumed to be the thickness of

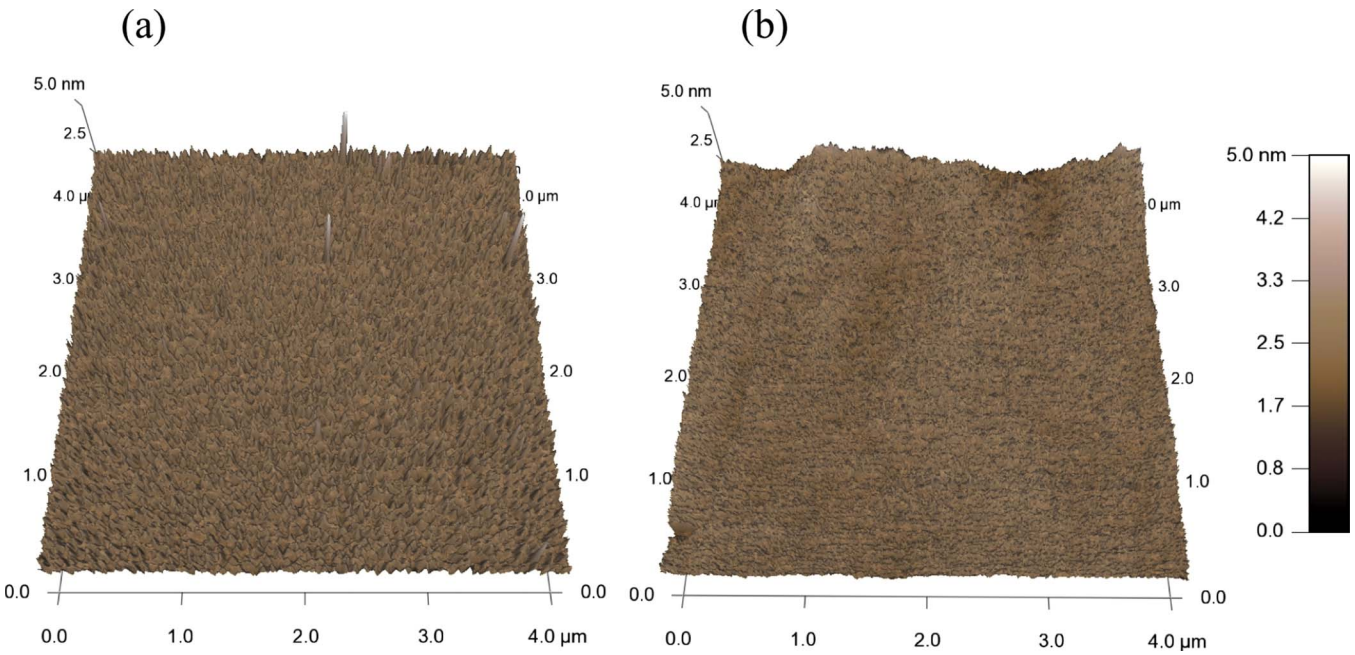

FIG. 4. (Color online) AFM images of PMP1$_{50}$ modified substrates (pH 6) dry (a) and wet (b).

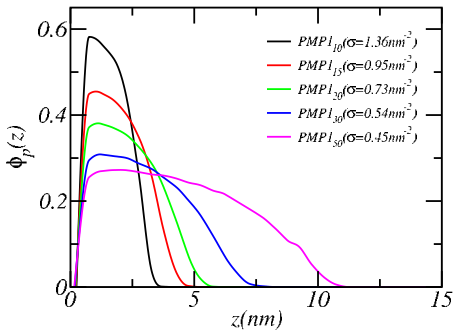

FIG. 5. (Color online) Volume fraction profile (segmental density distribution) of the polypeptoids as a function of the distance from the surface. The different conditions correspond to the amount of polypeptoid adsorbed experimentally with the values as marked in the legend.

the polymer coating. The experiments were repeated for the same surfaces after drying with N_2. The average dry thickness for $PMP1_{50}$ is 5.2 ± 0.3 nm, and the average thickness under aqueous conditions is 10.4 ± 0.8 nm, suggesting a doubling of polymer thickness when hydrated. Using similar AFM imaging methods, Harbers *et al.*[11] reported a dry film thickness of 10–20 nm and a hydrated film thickness of 50–100 nm for PEG coatings on glass. Using the contour length for amino acids (0.34 nm/residue), the calculated maximum thickness for $PMP1_{50}$ is 17 nm. Taking into account this calculated thickness, a hydrated surface thickness of 10 nm is quite plausible.

We can get more detailed information on the structure of the grafted peptoids by looking at the predictions of the molecular theory for the volume fraction profile of the peptoid for the measured surface coverage of polymers. This is shown in Fig. 5 for the five different polymers at the experimentally measured surface coverages. The peptoid segment profile shows a depletion region very close to the surface due to the presence of the adsorbed pentapeptide. The profiles show a stretched configuration with high local densities due to the bulky nature of the peptoid side groups. Interestingly, the local volume fraction in the region of maximal density is higher for the short polypeptoids. However, the films are thicker as the chain length increases. One can understand these two features by recalling that the strength of the binding to the surface is the same for all the different polymers. Therefore, the total repulsion between the peptoids at equilibrium needs to be the same. This is achieved by packing more polymers of short chain length with higher local segmental density. Note that this is a simple explanation since the full calculation also accounts for the loss of conformational entropy, which is a strong function of the chain length. Interestingly, the structure of the $PMP1_{50}$ predicted by the theory corresponds to a thickness slightly larger than 10 nm, in excellent agreement with the AFM observations. As we will discuss below, the structure of the different polymer layers is directly responsible for the nonfouling capabilities of the film.

TABLE III. Average protein-adsorption values with standard deviations for serum and lysozyme adsorption measured by OWLS.

	Adsorbed mass (ng/cm^2)	
Substrate	Serum	Fibrinogen
Bare TiO_2	342 ± 21	521 ± 61
$PMP1_{10}$	51 ± 7	4 ± 2
$PMP1_{15}$	53 ± 38	11 ± 2
$PMP1_{20}$	15 ± 15	7 ± 3
$PMP1_{30}$	28 ± 10	3 ± 3
$PMP1_{50}$	34 ± 13	4 ± 3
Tyr-$PMP1_{10}$	187 ± 77	319 ± 103

B. Resistance to protein adsorption

OWLS was also used for short-term protein-adsorption experiments with fibrinogen and human serum; the results are shown in Table III. Protein adsorption values on unmodified TiO_2 sensors were comparable to published OWLS data for serum[12] and fibrinogen;[58] protein adsorption results on all PMP1-modified sensors were significantly lower ($p < 0.05$) than unmodified TiO_2, but no statistically significant differences were observed between the PMP1-modified surfaces. The adsorbed serum masses for all PMP1-modified surfaces are similar to values for PEG coatings[8,10,12,17] and other PMP coatings.[36] Fibrinogen adsorption on the polymer-modified substrates is near to the ~ 5 ng/cm^2 threshold, below which activation of the pathways for blood coagulation does not occur,[12] suggesting possible use of the coatings for blood contacting applications where prevention of thrombosis is desired. Serum and fibrinogen adsorption values on the Tyr-$PMP1_{10}$-modified sensors were significantly greater than the values for PMP1-modified sensors, as was expected based on the thinner polymer coating. PMP1 chain lengths of 10–50 repeat units are equally suited for short-term protein resistant surfaces, but further experiments are necessary to predict long-term resistance. According to Fang *et al.*,[41] increasing the polymer chain length slows the adsorption kinetics for proteins; thus protein adsorption on the different polymers may not be seen until much longer time scales (months to years).

The experimental observations for each polypeptoid length correspond to one value of the polymer surface coverage. To obtain a better understanding of how the polymers prevent protein adsorption, we present calculations for the whole adsorption isotherms for each polypeptoid length. Figure 6 displays the amount of fibrinogen adsorbed as a function of the amount of polypeptoid on the surface. For each chain length of polypeptoid, increasing the polymer surface coverage reduces the amount of protein adsorbed. Furthermore, for each polypeptoid length, there is an amount of grafted polymer, above which there is no more protein adsorption. The critical surface coverage for nonfouling decreases as the polymer chain length increases in the range of chain length used in the experimental observations, i.e., up to $PMP1_{50}$. We have also included in the figure the predictions

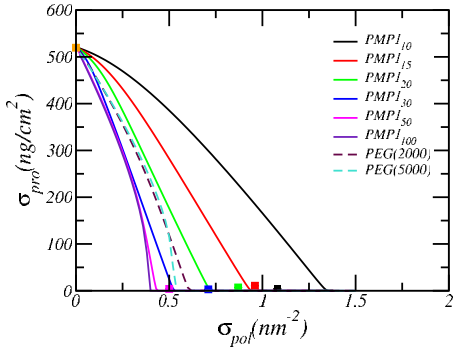

FIG. 6. (Color online) Protein-adsorption isotherms. The amount of fibrinogen adsorbed as a function of the surface coverage of end-tethered polypeptoid. The lines correspond to the theoretical predictions, while the symbols are the experimental observations. The point at $\sigma_{pol}=0$ corresponds to the bare TiO_2 surface.

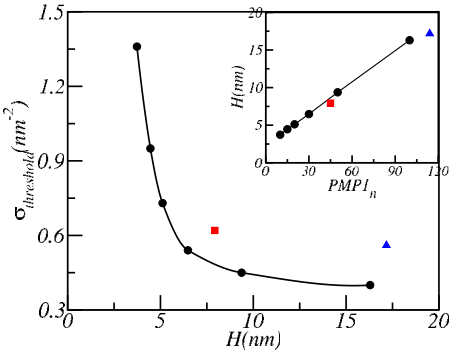

FIG. 7. (Color online) Calculated threshold surface coverage for fibrinogen adsorption as a function of the polymer layer thickness for polypeptoids (black circles), PEG-2000 (red square), and PEG-5000 (blue triangle). The inset shows the calculated thickness as a function of the chain length for the same polymers, all at the threshold surface coverage.

for $PMP1_{100}$, which has not been studied experimentally. The ability of this long polymer to prevent protein adsorption is almost identical to that of $PMP1_{50}$. This is very much in line with previous predictions for model PEG that predict that once the polymer film thickness is larger than the size of the protein the polymer chain length has no effect on the *equilibrium* adsorption isotherm;[50] however, it may have a very strong effect on the kinetics. As can be seen in Fig. 5, $PMP1_{30}$ forms a layer of thickness similar to the largest domain of fibrinogen, 6.5 nm. Thus, we expect that for polypeptoids with more than around 30–40 peptoids, the adsorption isotherm will be only weakly dependent on polymer size, as shown in Fig. 6.

In order to show the differences between polypeptoids and PEG, Fig. 6 shows the adsorption of fibrinogen as a function of surface coverage also for PEG-2000 and PEG-5000. In both cases, the ability of PEG to prevent protein adsorption at all surface coverages is less efficient than the polypetoids with more than 20 units. Moreover, the predicted threshold for complete prevention of protein adsorption is above the surface coverage achieved with PLL-*g*-PEG of 0.5 and 0.3 chains/nm^2 for PEG-2000 and PEG-5000, respectively. Thus, we expect the nonfouling capabilities of these PEG layers to be time dependent.

All these results can be explained in terms of the ability of the flexible polypeptoid to reduce and reject protein adsorption due to the effective steric interactions that result from the excluded volume repulsions combined with the reduction in the available number of polymer conformations when proteins adsorb. This also explains the more effective capabilities of the polypeptoids as compared to PEG, for the same number of units, since the peptoids are bulkier than the ethylene oxide units, and therefore, offer more steric repulsion on a per unit basis.

It is important to emphasize that the calculations represent equilibrium predictions. Namely, the theory assumes that the system has reached the thermodynamic preferred state of the system. However, it is not clear that the experimental observations, which are carried out over a relatively short time, reach the equilibrium state. Having this consideration, we see that for all the experimental polypeptoids, except $PMP1_{10}$, the amount of polymer bound to the surface is larger than what is necessary for the complete thermodynamic prevention of protein adsorption, and indeed the measured amount of protein adsorption (shown as symbols in Fig. 6) is close to zero.

The case of $PMP1_{10}$ is clearly different. The predicted isotherm shows that at the surface density of the experiment there will be a finite amount of adsorbed fibrinogen at equilibrium. However, the experimental observations show no adsorption. We return to this point later when we discuss cell adhesion on $PMP1_{10}$ covered surfaces.

An important prediction from the theory is the chain length dependence of the threshold surface coverage to completely prevent protein adsorption. Figure 7 shows the threshold surface coverage as a function of the film thickness, with the inset showing the film thickness as a function of polymer length. The thickness is calculated as $H=2\int\phi_{pol}(z)zdz/\int\phi_{pol}(z)dz$, which corresponds to the first moment of the polymer volume fraction profile. The thickness at the threshold surface coverage is linear with the polypeptoid chain length. Furthermore, the surface coverage threshold decreases very sharply for small thickness, but it levels off once the film thickness of the order of the protein size, in agreement with earlier predictions for PEG.[50] These results show that molecular weight dependence for the equilibrium amount of protein adsorption is not very large once the polymer thickness is larger than the size of the protein; however, one needs to keep in mind that this weak dependence does not hold for the kinetics of protein adsorption, where both surface coverage and molecular weight play very important roles.[41]

C. Resistance to mammalian cell adhesion

For cell adhesion studies, bare TiO_2 and polymer-modified TiO_2 substrates were seeded twice weekly with fresh 3T3 fibroblasts suspended in serum containing media. Cell attachment was quantified weekly for up to 7 weeks by live cell staining, fluorescence microscopy, and image analy-

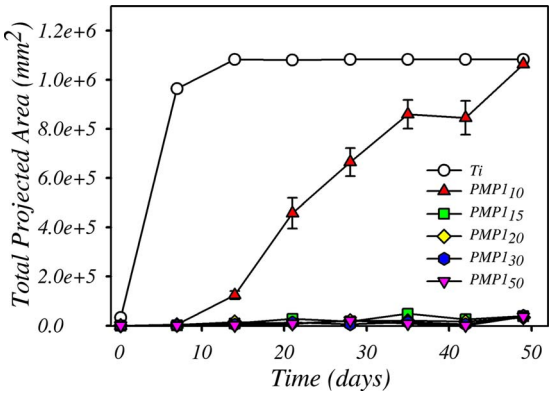

FIG. 8. (Color online) Total projected area of 3T3 fibroblasts during long-term cell culture on unmodified TiO_2, Tyr-$PMP1_{10}$, and $PMP1_n$ modified TiO_2 substrates.

sis (Fig. 8). At the initial 4 h time point, fibroblasts attached readily to the unmodified TiO_2 substrates and the Tyr-$PMP1_{10}$-modified substrates, while all $PMP1_n$-modified substrates were highly resistant to adhesion. Fibroblasts formed confluent monolayers on the unmodified TiO_2 substrates and the Tyr-$PMP1_{10}$-modified substrates by day 14. The $PMP1_{10}$-modified substrates initially exhibited low levels of cell attachment but demonstrated a steady increase in adhesion, reaching confluent monolayers by week 7. All other $PMP1_n$-modified substrates remained highly resistant to fibroblast adhesion throughout the experiment, which was expected for the 20-mer and longer chain lengths based on our previously reported 5-month study.[37]

The apparent threshold for long-term (7 weeks) fouling resistance is around 15 peptoid repeat units, which correlates to a dry polymer thickness of 32.5 ± 4.3 Å from ellipsometry experiments and an adsorbed polymer mass of 412.0 ± 67.6 ng/cm^2 from OWLS experiments. We can infer from these results that protein adsorption on polypeptoid polymers increases on time scales from months to years; therefore, if the 10-mer substrate was fouled by cells (and assumingly proteins) within 7 weeks in *in vitro* culture, we could predict that the 15-mer polymer would become fouled next, followed subsequently by the longer chain lengths. However, the theoretical predictions, see below, show that for the experimental surface coverages the nonfouling capability of the surfaces with 15-mer polymer (and longer) are time independent, i.e., equilibrium. Importantly, our cell adhesion results also support the previous claim that short-term (minutes to hours) protein-adsorption experiments may not always be the most reliable predictors of long-term (days, months, and years) biofouling events.[36,41]

We can make a more accurate prediction of protein (and cell) surface fouling by using the theoretical results presented in Fig. 6. According to the predictions, only $PMP1_{10}$ is tethered at a surface coverage lower than the minimal needed for thermodynamic prevention of protein adsorption. Therefore, that surface should foul, as demonstrated in experiments. The time scale for fouling can be determined as shown in earlier work,[41] and the time scale of days is not surprising. The predictions in Fig. 6 also show that none of the other surfaces should foul within the time frame of the current experiments since they are in the regime where thermodynamic control of protein adsorption is achieved. We thus believe that in those cases biofouling will not occur even in very long time scales.

IV. CONCLUSIONS

Polypeptoid polymers, composed of a peptide anchor coupled to *N*-methoxyethyl glycines of varying repeat lengths, were determined to have significant antifouling properties when immobilized onto TiO_2 substrates. A minimum chain length of 15 peptoids was demonstrated to be necessary for long-term (7 weeks) cell fouling resistance, suggesting that shorter polymer chain lengths do not provide sufficient coatings to prevent adsorption of proteins to the underlying substrates for longer time scales.

The use of a predictive molecular theory can be a very important component in the design of surface modifiers for nonfouling applications. We have shown that the theory enables the prediction of the amount of polypeptoid bound to the surface and the ability of that surface to prevent protein adsorption. The optimal conditions for modification are such that the bound surface coverage is larger than the minimal coverage needed for *thermodynamic* prevention of protein adsorption. If the tethered polymers are at lower surface densities, long-term fouling will occur. The compromise between surface coverage and molecular weight in determining fouling capabilities depends on the chemical nature of the polymers and can be determined *a priori* with the theoretical tools.

ACKNOWLEDGMENTS

This research was supported by NIH Grant Nos. EB005772 and DE014193. XPS surface analysis was performed at KeckII/NU*ANCE* at Northwestern University. Mass spectrometry was completed at the Northwestern University Analytical Services Laboratory. The authors thank Haeshin Lee for the assistance with AFM and XPS experiments and many discussions.

[1] J. L. Brash, J. Biomater. Sci., Polym. Ed. **11**, 1135 (2000).
[2] T. A. Horbett, Cardiovasc. Pathol. **2**, Supplement 1, 137 (1993).
[3] B. D. Ratner, J. Biomed. Mater. Res. **27**, 283 (1993).
[4] N. Wisniewski and M. Reichert, Colloids Surf., B **18**, 197 (2000).
[5] J. D. Bryers, Colloids Surf., B **2**, 9 (1994).
[6] G. G. Geesey and J. D. Bryers, in *Biofilms II*, edited by J. D. Bryers (Wiley-Liss, New York, 2000), pp. 237–279.
[7] J. P. Bearinger, D. G. Castner, S. L. Golledge, S. Hubchak, and K. E. Healy, Langmuir **13**, 5175 (1997).
[8] J. P. Bearinger, S. Terrettaz, R. Michel, N. Tirelli, H. Vogel, M. Textor, and J. A. Hubbell, Nature Mater. **2**, 259 (2003).
[9] J. L. Dalsin, B. H. Hu, B. P. Lee, and P. B. Messersmith, J. Am. Chem. Soc. **125**, 4253 (2003).
[10] J. L. Dalsin, L. Lin, S. Tosatti, J. Voros, M. Textor, and P. B. Messersmith, Langmuir **21**, 640 (2005).
[11] G. M. Harbers, K. Emoto, C. Greef, S. W. Metzger, H. N. Woodward, J. J. Mascali, D. W. Grainger, and M. J. Lochhead, Chem. Mater. **19**, 4405 (2007).
[12] G. L. Kenausis, J. Voros, D. L. Elbert, N. Huang, R. Hofer, L. Ruiz-Taylor, M. Textor, J. A. Hubbell, and N. D. Spencer, J. Phys. Chem. B

104, 3298 (2000).
[13]H. W. Ma, J. H. Hyun, P. Stiller, and A. Chilkoti, Adv. Mater. (Weinheim, Ger.) **16**, 338 (2004).
[14]M. Malmsten, K. Emoto, and J. M. Van Alstine, J. Colloid Interface Sci. **202**, 507 (1998).
[15]S. Pasche, S. M. De Paul, J. Voros, N. D. Spencer, and M. Textor, Langmuir **19**, 9216 (2003).
[16]S. J. Sofia, V. Premnath, and E. W. Merrill, Macromolecules **31**, 5059 (1998).
[17]N. Xia, Y. Hu, D. W. Grainger, and D. G. Castner, Langmuir **18**, 3255 (2002).
[18]D. A. Herold, K. Keil, and D. E. Bruns, Biochem. Pharmacol. **38**, 73 (1989).
[19]F. Kawai, Appl. Microbiol. Biotechnol. **58**, 30 (2002).
[20]F. Kawai, T. Kimura, M. Fukaya, Y. Tani, K. Ogata, T. Ueno, and H. Fukami, Appl. Environ. Microbiol. **35**, 679 (1978).
[21]S. Sharma, R. W. Johnson, and T. A. Desai, Langmuir **20**, 348 (2004).
[22]S. Han, C. Kim, and D. Kwon, Polymer **38**, 317 (1997).
[23]H. Bi, W. Zhong, S. Meng, J. Kong, P. Yang, and B. Liu, Anal. Chem. **78**, 3399 (2006).
[24]M. Casolaro, S. Bottari, and Y. Ito, Biomacromolecules **7**, 1439 (2006).
[25]S. J. Dilly, M. P. Beecham, S. P. Brown, J. M. Griffin, A. J. Clark, C. D. Griffin, J. Marshall, R. M. Napier, P. C. Taylor, and A. Marsh, Langmuir **22**, 8144 (2006).
[26]W. Feng, S. Zhu, K. Ishihara, and J. L. Brash, Langmuir **21**, 5980 (2005).
[27]T. Ishii, A. Wada, S. Tsuzuki, M. Casolaro, and Y. Ito, Biomacromolecules **8**, 3340 (2007).
[28]R. Iwata, P. Suk-In, V. P. Hoven, A. Takahara, K. Akiyoshi, and Y. Iwasaki, Biomacromolecules **5**, 2308 (2004).
[29]S. L. West, J. P. Salvage, E. J. Lobb, S. P. Armes, N. C. Billingham, A. L. Lewis, G. W. Hanlon, and A. W. Lloyd, Biomaterials **25**, 1195 (2004).
[30]H. J. Griesser, P. G. Hartley, S. McArthur, K. M. McLean, L. Meagher, and H. Thissen, Smart Mater. Struct. **11**, 652 (2002).
[31]N. B. Holland, Y. Qiu, M. Ruegsegger, and R. E. Marchant, Nature (London) **392**, 799 (1998).
[32]S. L. McArthur, K. M. McLean, P. Kingshott, H. A. W. St John, R. C. Chatelier, and H. J. Griesser, Colloids Surf., B **17**, 37 (2000).
[33]E. Österberg, K. Bergström, K. Holmberg, T. P. Schuman, J. A. Riggs, N. L. Burns, J. M. Van Alstine, and J. M. Harris, J. Biomed. Mater. Res. **29**, 741 (1995).
[34]M. A. Ruegsegger and R. E. Marchant, J. Biomed. Mater. Res. **56**, 159 (2001).
[35]R. Konradi, B. Pidhatika, A. Muhlebach, and M. Textor, Langmuir **24**, 613 (2008).
[36]A. R. Statz, A. E. Barron, and P. B. Messersmith, Soft Matter **4**, 131 (2008).
[37]A. R. Statz, R. J. Meagher, A. E. Barron, and P. B. Messersmith, J. Am. Chem. Soc. **127**, 7972 (2005).
[38]D. O. Teare, W. C. Schofield, R. P. Garrod, and J. P. Badyal, J. Phys. Chem. B **109**, 20923 (2005).
[39]J. H. Waite and X. Qin, Biochemistry **40**, 2887 (2001).
[40]J. H. Waite and M. L. Tanzer, Science **212**, 1038 (1981).
[41]F. Fang, J. Satulovsky, and I. Szleifer, Biophys. J. **89**, 1516 (2005).
[42]J. Satulovsky, M. A. Carignano, and I. Szleifer, Proc. Natl. Acad. Sci. U.S.A. **97**, 9037 (2000).
[43]I. Szleifer, Biophys. J. **72**, 595 (1997).
[44]R. N. Zuckermann, J. M. Kerr, S. B. H. Kent, and W. H. Moos, J. Am. Chem. Soc. **114**, 10646 (1992).
[45]J. N. Hilfiker and R. A. Synowicki, Solid State Technol. **41**, 101 (1998).
[46]J. A. de Feijter, J. Benjamins, and F. A. Veer, Biopolymers **17**, 1759 (1978).
[47]J. H. Scofield, J. Electron Spectrosc. Relat. Phenom. **8**, 129 (1976).
[48]I. Szleifer, Curr. Opin. Colloid Interface Sci. **1**, 416 (1996).
[49]T. McPherson, A. Kidane, I. Szleifer, and K. Park, Langmuir **14**, 176 (1998).
[50]F. Fang and I. Szleifer, Langmuir **18**, 5497 (2002).
[51]I. Szleifer, Physica A **244**, 370 (1997).
[52]See EPAPS Document No. E-BJIOBN-4-003902 for HPLC and MALDI-MS characterization of polypeptoids. For more information on EPAPS, see http://www.aip.org/pubservs/epaps.html.
[53]J. M. Harris and S. Zalipsky, *American Chemical Society, Division of Polymer Chemistry and American Chemical Society Meeting* (American Chemical Society, Washington, DC, 1997).
[54]P. Kingshott, H. Thissen, and H. J. Griesser, Biomaterials **23**, 2043 (2002).
[55]H. Lee, N. F. Scherer, and P. B. Messersmith, Proc. Natl. Acad. Sci. U.S.A. **103**, 12999 (2006).
[56]R. Kurrat, B. Walivaara, A. Marti, M. Textor, P. Tengvall, J. J. Ramsden, and N. D. Spencer, Colloids Surf., B **11**, 187 (1998).
[57]J. Voros, J. J. Ramsden, G. Csucs, I. Szendro, S. M. De Paul, M. Textor, and N. D. Spencer, Biomaterials **23**, 3699 (2002).
[58]F. Hook, J. Voros, M. Rodahl, R. Kurrat, P. Boni, J. J. Ramsden, M. Textor, N. D. Spencer, P. Tengvall, J. Gold, and B. Kasemo, Colloids Surf., B **24**, 155 (2002).